Computational and Structural Biotechnology Journal 20 (2022) 3946–3954

COMPUTATIONAL ANDSTRUCTURAL BIOTECHNOLOGY JOURNAL

journal homepage: www.elsevier.com/locate/csbj

# Ceftazidime-avibactam based combinations against carbapenemase producing *Klebsiella pneumoniae* harboring hypervirulence plasmids

Zackery P. Bulman [a,*], Xing Tan [a], Ting-Yu Chu [b], Yanqin Huang [a], Amisha P. Rana [a], Nidhi Singh [a], Stephanie A. Flowers [a], Yasuhiro Kyono [a], Barry N. Kreiswirth [b,c], Liang Chen [b,c]

[a] Department of Pharmacy Practice, College of Pharmacy, University of Illinois Chicago, Chicago, IL, USA
[b] Center for Discovery and Innovation, Hackensack Meridian Health, Nutley, NJ, USA
[c] Department of Medical Sciences, Hackensack Meridian School of Medicine, Nutley, NJ, USA

ARTICLE INFO

*Article history:*
Received 6 April 2022
Received in revised form 8 July 2022
Accepted 8 July 2022
Available online 15 July 2022

*Keywords:*
Carbapenem-resistant
*Klebsiella pneumoniae*
Hypervirulent
Transcriptomic
Antibiotic tolerance

ABSTRACT

The combination of carbapenem resistance and hypervirulence in *Klebsiella pneumoniae* is an emerging and urgent threat due to its potential to resist common antibiotics and cause life-threatening infections in healthy hosts. This study aimed to evaluate the activity of clinically relevant antibiotic regimens against carbapenem-resistant *K. pneumoniae* with hypervirulence plasmids and to identify pathways associated with antibiotic tolerance using transcriptomics. We studied two carbapenem-resistant *K. pneumoniae* isolates, CDI694 and CDI231, both harboring hypervirulence plasmids. Time-kill and dynamic one-compartment pharmacokinetic/pharmacodynamic assays were used to assess ceftazidime/avibactam-based therapies. RNAseq was performed following 48 h of antibiotic exposure. Closed genomes of CDI694 and CDI231 were obtained; each isolate harbored carbapenem-resistance and hypervirulence (containing *rmpA/rmpA2* and *iut* genes) plasmids. Ceftazidime/avibactam-based regimens were bactericidal, though both isolates continued to grow in the presence of antibiotics despite no shifts in MIC. Transcriptomic analyses suggested that perturbations to cell respiration, carbohydrate transport, and stress-response pathways contributed to the antibiotic tolerance in CDI231. Genes associated with hypervirulence and antibiotic resistance were not strongly impacted by drug exposure except for *ompW*, which was significantly downregulated. Treatment of carbapenem-resistant *K. pneumoniae* harboring hypervirulence plasmids with ceftazidime/avibactam-based regimens may yield a tolerant population due to altered transcription of multiple key pathways.



## 1. Introduction

In Western countries, infections due to *Klebsiella pneumoniae* are primarily caused by classical *K. pneumoniae* (cKP) strains and manifest as opportunistic infections in patients with compromised immunity.[1,2] cKP strains have demonstrated a proclivity to acquire resistance mechanisms, including carbapenemases, but they are historically not considered hypervirulent.[3,4] In contrast, hypervirulent *K. pneumoniae* (hvKP) has been shown to cause metastatic infections among healthy hosts in the community. These infections are associated with mortality rates of up to ~40% and significant morbidity, including visual and neurological impairment.[5–7] Virulence in hvKP is primarily attributed to siderophore production and increased capsule polysaccharide (CPS).[8] Although infections caused by hvKP are associated with high rates of morbidity and mortality, these strains have historically retained high rates of susceptibility to antibiotics.[9,10].

Carbapenem-resistant hypervirulent *K. pneumoniae* (CR-hvKP) is an evolving pathotype of imminent threat to public health [9]. CR-hvKP is particularly problematic since it combines the ability to cause life-threatening infections within healthy hosts with resistance to a majority of the β-lactam antibiotics. Unfortunately, CR-hvKP has now been identified in countries around the world, elevating the need for the development infection control and antimicrobial treatment strategies.[11–14] Although a number of studies have evaluated antimicrobials against carbapenem-resistant cKP, there are no prospective clinical studies and limited *in vitro* studies evaluating the efficacy of antimicrobials against hvKP or CR-hvKP.[15–17] Based on the poor clinical outcomes after hvKP infections and *in vitro* data that suggest that antimicrobials can modulate CPS synthesis, it is possible that the CPS produced by hvKP strains

* Corresponding author.
*E-mail address:* bulman@uic.edu (Z.P. Bulman).

https://doi.org/10.1016/j.csbj.2022.07.017

affects the pharmacodynamics of antibacterial agents.[18–21] With only a few remaining antibiotics active against CR-hvKP, novel approaches urgently need to be defined.[22] The objective of this study was to identify active antibiotic regimens against carbapenem-resistant *K. pneumoniae* with hypervirulence plasmids and evaluate the bacterial transcriptomic response to therapy.

## 2. Methods

### 2.1. Bacterial strains and whole genome sequencing

Two representative carbapenem-resistant *K. pneumoniae* isolates with hypervirulence genes obtained from East Asia (CDI694) and the Middle East (CDI231) were used in this study (Table 1). These isolates are representative of the CR-hvKP strains that have emerged in patients, which have plasmids with hypervirulence and multidrug-resistance genes. They were also chosen based on their carbapenemase genes. One isolate with $bla_{KPC}$ (CDI694) and one isolate with $bla_{NDM}$ and $bla_{OXA-48}$ (CDI231) were selected. Hypervirulence was defined by the presence of the plasmid-borne *rmpA/rmpA2* (regulator of the mucoid phenotype A) and *iut* (aerobactin) genes.[2,8] Whole-genome sequencing was performed using a combination of the Illumina Hiseq platform and Oxford Nanopore Technologies (ONT) MinION sequencing. Briefly, DNA was isolated from overnight cultures using a MasterPure™ Gram Positive DNA Purification Kit as recommended by the manufacturer (Epicentre, USA). Illumina libraries were prepared for sequencing using NexteraXT kits and sequenced on a HiSeq platform with paired 150-base sequence reads. Nanopore libraries were prepared using Ligation Sequencing Kit (SQK-RBK109) and loaded onto an R9.4 flow cell and the run was performed on MinION Mk1B device. Hybrid assembly was conducted using Unicycler v0.4.9. with the default settings.[23] MICs were determined by broth microdilution in triplicate according to CLSI guidelines (Table 1).[24].

### 2.2. Time-kill assays

Static time-kill assays were performed against a starting inoculum of each isolate at $\sim 10^7$ cfu/mL, as previously described.[25,26] Aztreonam (ATM), ceftazidime (CAZ), avibactam (AVI), meropenem (MEM), minocycline (MIN), and polymyxin B (PMB) were obtained from Sigma-Aldrich, Inc. On the first day of each experiment, antibiotics were prepared at 50% and 100% of the estimated maximal serum achievable free-drug concentrations ($fC_{max}$), except ATM, which was prepared only at 100% $fC_{max}$, as it will not be active as monotherapy against these isolates.[27–31] Combinations with CAZ/AVI (at 50% and 100% $fC_{max}$) and another agent (at the highest concentration that was not bactericidal) were then tested to evaluate for synergy. CAZ/AVI in combination with ATM, MEM, MIN, or PMB, was tested against the CDI694 isolate, while CAZ/AVI + ATM alone, and in triple combination with MEM, MIN, or PMB, was tested against CDI231. Bacterial suspensions were prepared in cation-adjusted Mueller-Hinton broth (CAMHB, Becton Dickinson) and exposed to antibiotics for 24 h while being incubated at 37C with constant shaking. Viable bacterial cell counts were obtained at 0, 1, 2, 4, 6, 8, and 24 h. Bactericidal activity was defined as $\geq$ 3 $\log_{10}$cfu/mL reduction from the initial inoculum. Synergy was defined as a $\geq$ 2 $\log_{10}$cfu/mL decrease following exposure to the combination compared with the most active agent alone.

### 2.3. One-compartment Pharmacokinetic/pharmacodynamic model experiments

The most active and clinically relevant antibiotic regimens were further investigated in a dynamic one-compartment model to examine the effect of simulated human drug exposures over 48 h, as previously described.[26] Briefly, CAMHB was continuously pumped into sealed central reservoirs. The central reservoirs were threaded 250 mL Erlenmeyer flasks modified with a glass port for sampling and fitted with a reservoir cap (FiberCell Systems) that permits inflow of media and antibiotics as well as the simultaneous outflow of waste media. The flow rates in and out of the reservoir were identical to maintain a constant volume of media (105 mL) throughout the experiment. The flow rates were set to simulate the approximate half-lives of CAZ/AVI and ATM expected in patients ($\sim$2 h). The central reservoirs were placed on a multi-point stirrer in a 37 °C incubator with the bacteria at an inoculum of $\sim 10^7$ cfu/mL. A magnetic stir bar in the reservoirs was used to ensure constant mixing and homogeneity. Antibiotics were infused into the central reservoir via an automated syringe pump (NE-1600; New Era Pumps Systems) to simulate both "sub-therapeutic" (10%) and "average" (100%) human pharmacokinetic exposures. CAZ/AVI (for both strains) was administered to mimic a dose of 2.5 gm every 8 h ("average" regimen $fC_{max}$ of 75/15 mg/L) and ATM (for CDI231) was administered to mimic a dose of 2 gm every 8 h ("average" regimen $fC_{max}$ of 75 mg/L).[27,28] Each antibiotic dose (starting at 0, 8, 16, 24, 32, and 40 h) was infused for a duration of two hours. Viable bacterial cell counts were performed at 0, 2, 4, 6, 24, 25, 26, 28, 30, and 48 h after the start of drug administration. MICs were determined again for both isolates after 48 h of drug exposure.

### 2.4. RNA-sequencing (RNA-seq) and sequence analysis

To investigate the transcriptomic response in the CR-hvKP isolates that may permit them to persist during antibiotic therapy, RNA-seq was performed following antibiotic exposure in the one-compartment model for CDI231. Bacteria for transcriptomic analyses from control (no drug) and treated (100% CAZ/AVI + 100% ATM) samples were collected at the 48 h time point, flash frozen using liquid nitrogen, and then stored at −80 °C until RNA-seq was performed. To identify expression changes associated with persistence, the 48 h samples were used for RNA-seq since the bacteria from this time point were able to grow in the presence of antibiotics without increases in MIC. Total RNAs were extracted using the RNA Mini kit (Qiagen), followed by TURBO™ DNase (Invitrogen) treatment to clear DNA contamination. rRNA depletion was conducted by Ribo-Zero Plus rRNA Depletion Kit (Illumina), and the RNASeq libraries were generated by TruSeq® mRNA Library preparation kits, followed by sequencing in an Illumina NextSeq 500

**Table 1**
MICs of the CR-hvKP isolates.

| Isolate | MICs (mg/L) | | | | | | | |
|---|---|---|---|---|---|---|---|---|
| | ATM | ATM/CAZ/AVI | CAZ/AVI | CAZ | MEM | MIN | PMB | RIF |
| CDI694 | >64 | ≤0.5/8/4 | 4/4 | >64 | 128 | 8 | 0.25 | 16 |
| CDI231 | >64 | ≤0.5/8/4 | >64/4 | >64 | 16 | 2 | 0.25 | 16 |

ATM, aztreonam; CAZ, ceftazidime; CAZ/AVI, ceftazidime/avibactam; MEM, meropenem; MIN, minocycline; PMB, polymyxin B; RIF, rifampin.

platform with single end 75 bp reads. RNA-seq was performed in duplicate. The raw reads were filtered by trimmomatic v0.39,[32] and the filtered reads were mapped to the closed reference genome generated hybrid assembly using Bowtie2 v2.4.2 [33]. Read counting at each gene was generated by HTSeq v0.13.5,[34] and differential gene expression analysis was conducted by DESeq2 in R.[35] Gene ontology (GO) and KEGG orthology were predicted by eggnog-mapper v2.1.0 [36] and BlastKOALA v2.2,[37] respectively. The GO and KEGG enrichment was conducted using clusterProfiler in R.[38].

## 3. Results

### 3.1. hvKP whole genome sequences

The hybrid assembly using the combination of Illumina and Nanopore sequencing data successfully closed the two genomes of CDI231 and CDI694. They both carried one circular chromosome of 5,344,935 and 5,473,734 bps in length, respectively. They both harbored 5 circular plasmids, ranging from 9.29 to 348.3 kb in CDI231, and 5.6 to 216.6 kb in CDI694. CDI231 belonged to ST377 with KL102 capsular type, while CDI694 was an ST11 strain of KL64 capsular type.

In CDI694, $bla_{KPC-2}$ and $bla_{CTX-M-65}$ were harbored on an IncFII (pHN7A8)-R plasmid (pCDI694-140.8) of 140,828 bp in length (Fig. S1). CDI694 harbored an IncHIB-FIB pLVPK-like virulence plasmid, pCDI694-216.6, carrying the salmochelin (*iro*), aerobactin (*iuc*) gene clusters and the *rmpA*, *rmpA2* (truncated) genes (Fig. 1).

In CDI231, $bla_{OXA-48}$ is harbored on a 63.6 kb IncL pOXA-48a-like plasmid (pCDI231-63.6), of which $bla_{OXA-48}$ is located in a Tn*1999.2* element (Fig. S1). The sequence of pCDI231-63.6 was identical to a number of plasmids isolated from Switzerland (e.g. CP039947), Russia (e.g. CP063280), Netherlands (e.g. CP068298), India (e.g. CP076010) and Spain (e.g. MT989343) from *K. pneumoniae*, *E. coli*, and *Citrobacter freundii*. The $bla_{NDM-1}$ gene was carried on a large 348.3 Kb IncHIB-FIB plasmid, pCDI231-348.3, which showed >99% query coverage and >99.9% sequence identities to plasmid p51015_NDM_1 (CP050380) and phvKpST147_NDM1_1659 (CP072810) from Czech Republic and Russia, respectively (Fig. 1). $bla_{NDM-1}$ was located in a ~47 kb region, co-harboring *aph(3′)-la*, *aph(3′)-VI*, *armA*, *mph(A)*, *mph(E)*, *msr(E)*, *qnrS1*, *sul1*, *sul2*, and *dfrA5* genes, and conferring resistance to some aminoglycosides, macrolides, fluoroquinolones, sulfonamides and trimethoprim. pCDI231-348.3 also carry the virulence genes *rmpA*, *rmpA2* (truncated) and aerobactin encoding gene clusters (*iuc*) (Fig. 1).

### 3.2. Time-kill assays

In the time-kill assays, the only bactericidal monotherapy was CAZ/AVI against CDI694, which caused 3.2 and 3.7 $\log_{10}$cfu/mL reductions at the 50% and 100% $fC_{max}$ concentrations, respectively (Fig. 2A). At 24 h, all other monotherapies against CDI694 and each monotherapy against CDI231 had viable counts near growth control (i.e. no reduction at 24 h) (Fig. 2C). While not bactericidal, PMB monotherapy did initially result in a >2 $\log_{10}$cfu/mL bacterial reduction at 8 h against both isolates but was followed by subsequent regrowth. No combinations with CAZ/AVI were synergistic against CDI694 (Fig. 2B), while combinations with CAZ/AVI + ATM were found to be synergistic against CDI231 (Fig. 2D). Against CDI231, CAZ/AVI + ATM combinations led to decreases of 2.4 (CAZ/AVI 50% $fC_{max}$) and 3.4 (CAZ/AVI 100% $fC_{max}$) $\log_{10}$cfu/mL. Triple combination therapy with CAZ/AVI + ATM + PMB resulted in bacterial reductions of 4.4 (CAZ/AVI 50% $fC_{max}$) and 4.5 (CAZ/AVI 100% $fC_{max}$) $\log_{10}$cfu/mL against CDI231.

### 3.3. One-compartment pharmacokinetic/pharmacodynamic model

In the one-compartment model, the 10% and 100% CAZ/AVI 2.5 gm q8h regimens alone against CDI694 showed initial killing at 6 h of 2.6 and 3.0 $\log_{10}$cfu/mL, respectively (Fig. 3A). However, initial killing was not sustained, and regrowth occurred at 48 h with the 10% regimen, while the 100% regimen was approximately static from 6 to 48 h. Only a 1 dilution increase in CAZ/AVI MIC was observed for CDI694 after 48 h of treatment (Table 2). Against CDI231, initial killing of ~2–3 $\log_{10}$cfu/mL caused by the CAZ/AVI 2.5 gm q8h + ATM 2 gm q8h regimens was sustained through 26 h (Fig. 3B). Regrowth was observed for the 10% regimen by 48 h whereas the 100% regimen yielded a final reduction of 1.74 $\log_{10}$cfu/mL. Similar to CDI694, no increase in MIC was observed in CDI231 after 48 h of treatment (Table 2).

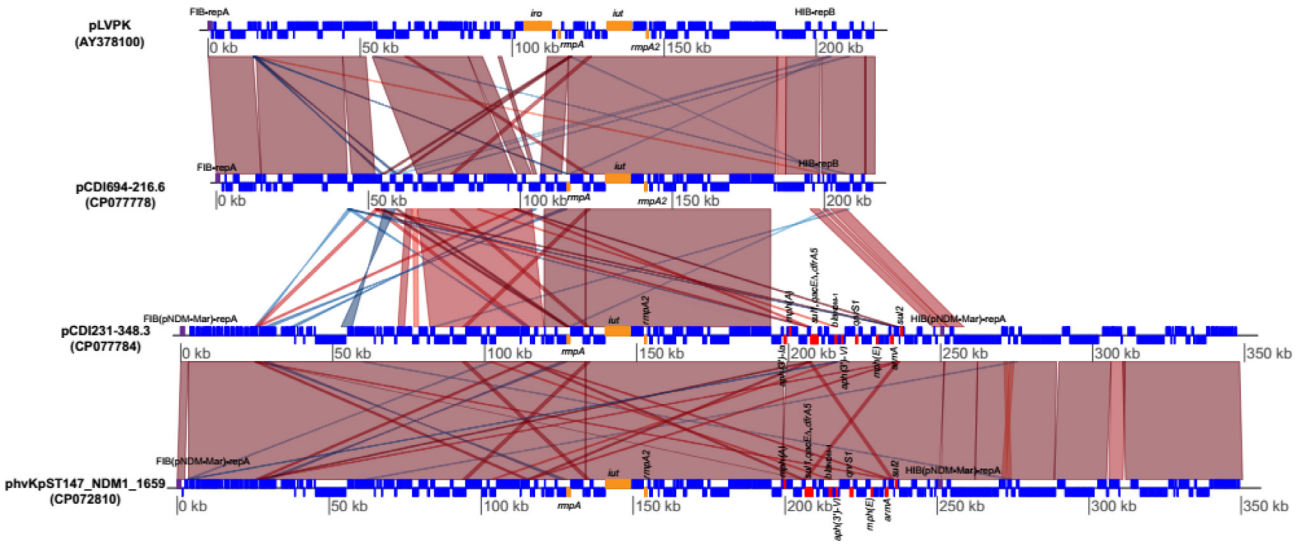


**Fig. 1.** Structures of hypervirulent plasmids pLVPK, pCDI694-216.6, pCDI231-348.3 and phvKpST147_NDM1_1659. The virulence genes *rmpA*/*rmpA2*, *iut*, *iro* appear highlighted in yellow, while antimicrobial resistance genes appear highlighted in red. (For interpretation of the references to colour in this figure legend, the reader is referred to the web version of this article.)

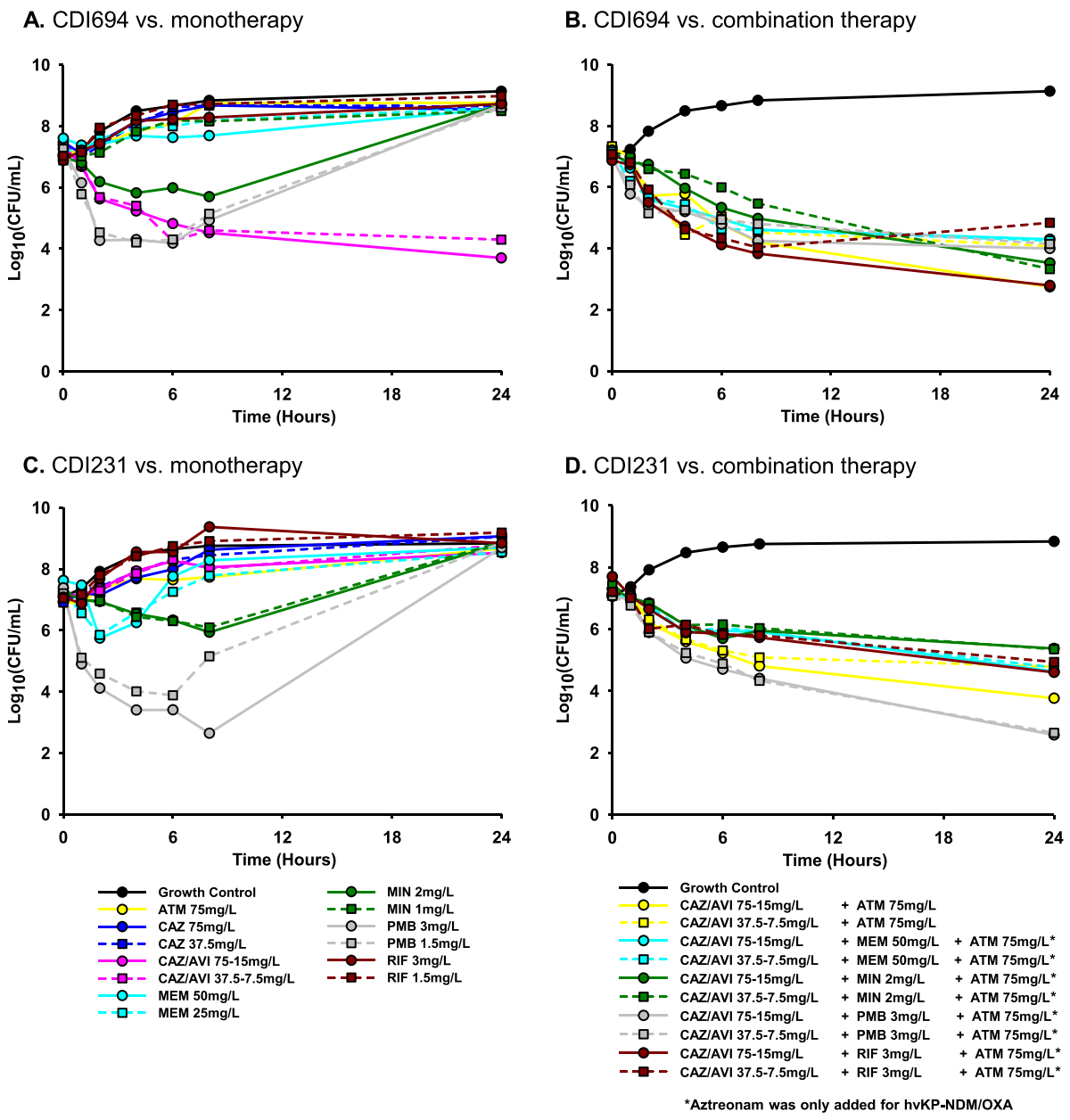


**Fig. 2.** Bacterial killing by monotherapy and combination therapy in time-kill experiments against CDI694 (A and B) and CDI231 (C and D).

### *3.4. RNA-sequencing (RNA-seq)*

Despite achieving antibiotic concentrations in excess of the MIC, the drug regimens failed to eradicate either hvKP isolate in the one-compartment model. After drug exposure, there were no changes to the MIC suggesting the isolates could sustain growth in the presence of antibiotic through mechanism(s) other than resistance development. To study this persistence, we performed RNA-seq to assess the transcriptomic response of CDI231 to CAZ/AVI and ATM (100% doses).

#### *3.4.1. Differentially expressed genes (DEGs)*

There were a total of 513 DEGs that had a $\log_2$ fold change of >2 or <−2 with a false discovery rate of <0.01 in CDI231 exposed to CAZ/AVI and ATM for 48 h. Among these, 431 genes were downregulated and 82 were upregulated (Fig. 4A). GO enrichment analysis showed that the genes most significantly perturbed by antibiotic exposure in CDI231 were related to: 1) generation of energy/respiration, 2) carbohydrate transport, 3) stress response, 4) detoxification/antioxidant activity, 5) threonine/cofactor catabolism, and 6) cell metabolism (Fig. 4B and C). There were 64 unique DEGs related to the generation of energy/respiration GO terms; 56 were downregulated and 8 upregulated. Within this group, the genes (product) that displayed the greatest change in expression were *tdcD* (propionate kinase), *katG* (catalase peroxidase), *ahpF* (alkyl hydroperoxide reductase), and *frdA* (fumarate reductase flavoprotein subunit) with −6.63, −5.84, −5.56, and −5.36 $\log_2$ fold change compared to non-antibiotic exposed bacteria, respectively. In addition to *frdA*, the whole fumarate reductase operon (*frdABCD*), which encodes an enzyme that converts fumurate to succinate, was downregulated upon antibiotic exposure as were *fumA* and *fumB*. The *fumA* and *fumB* genes encode fumarase enzymes that are involved in the tricarboxylic acid cycle and catalyze the reversible conversion of fumarate to malate. Genes encoding glycerol-3-phosphate dehydrogenase that act under anaerobic (*glpABC*) and aerobic (*glpD*) conditions were significantly downregulated

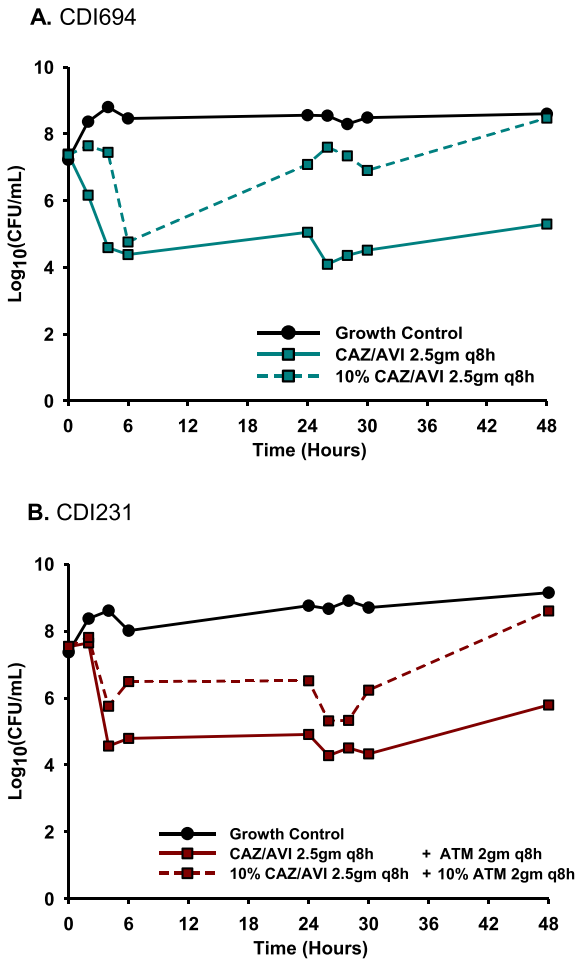


**Fig. 3.** Pharmacodynamic activity of CAZ/AVI against CDI694 (A) and CAZ/AVI in combination with ATM against CDI231 (B) in the one-compartment model.

(−3.00 to −3.50 $\log_2$ fold) and upregulated (2.86 $\log_2$ fold), respectively.

There were 22 DEGs related to carbohydrate transport; 21 were downregulated and 1 was upregulated. Among genes related to carbohydrate transport, the genes (product) that displayed the greatest change in expression were *lamB* (maltoporin), *malE* (maltose-binding periplasmic protein), and *malK* (maltose/maltodextrin import ATP-binding protein) with −5.57, −5.24, and −4.42 $\log_2$ fold change compared to non-antibiotic exposed bacteria, respectively. The *malE* and *malK* genes encode portions of the ABC maltose transporter; the other two subunits of this transporter (*malF* and *malG*) were also significantly repressed following antibiotic exposure. Genes related to the quorum sensing autoinducer 2 (AI-2) ATP-binding cassette transporter system were also found to have decreased expression (*lsrABCD*). Further, the *manXYZ* operon, which encodes three proteins that form the phosphoenolpyruvate-dependent phosphotransferase (PTS) system that transports mannose, was also significantly downregulated.

Various stress response genes were also perturbed following exposure to CAZ/AVI and ATM. There were 66 DEGs related to stress response; 61 were downregulated and 5 were upregulated. Within stress response genes, seven displayed <−5 $\log_2$ fold change compared to non-antibiotic exposed bacteria including *katG*, *dps* (DNA protection during starvation protein), *lamB*, *ychH* (stress-induced protein), *frdA*, *malE, btsT* (pyruvate/proton symporter), and *cstA* (carbon starvation protein A). Most $H_2O_2$-scavenger encoding genes were not upregulated and, in fact, many were significantly downregulated (*ahpC, ahpF, katE,* and *katG*). Superoxide dismutase genes, which encode for enzymes that convert superoxide radicals to oxygen and $H_2O_2$, were both up- (*sodA*) and down- (*sodB, sodC*) regulated. Another notable stress response gene, *rpoS*, was also downregulated but did not meet the <−2 $\log_2$ fold change threshold while the DNA repair gene *recA* was not differentially expressed.

### *3.4.2. Differentially expressed hypervirulence and β-lactam resistance genes*

Since these isolates were multidrug-resistant and hypervirulent, we also specifically looked at the transcription of genes previously described to be associated with these phenotypes. For these genes, DEGs were defined as having a $\log_2$ fold change of >1 or <−1 with a false discovery rate of <0.05. Following exposure to CAZ/AVI and ATM, 5 DEGs in CDI231 that may be associated with hypervirulence were identified (Table 3). Three of these genes (*peg-589, rmpA,* and *galF*) were down-regulated while two were upregulated (*iucB* and *iucD*). There were 4 DEGs that have previously been linked with β-lactam resistance including 2 β-lactamase genes (2 other β-lactamase genes were not differentially expressed) and 2 relating to drug permeability (Table 3). The β-lactamases were down-regulated as were both outer membrane protein DEGs. One of these outer membrane protein genes (*ompW*) had a $\log_2$ fold change of <−6.0.

## 4. Discussion

The evolutionary merge of the hypervirulent phenotype with a variety of antibiotic resistance mechanisms within *K. pneumoniae* holds the potential to cause widespread devastating and untreatable disease.[22] The most common CR-hvKP in China is currently the KPC-2-producing K64-ST11 strain, though isolates harboring other carbapenemases, including metallo- and OXA-type β-lactamases, have also been identified worldwide.[11,39–43] Despite increasing prevalence, limited data are available to guide treatment of CR-hvKP infections. The present study showed that CAZ/AVI and CAZ/AVI + ATM were active against CDI694 and

**Table 2**
MICs of CR-hvKP isolates after 48 h antibiotic exposures in the one-compartment model.

| Isolate | Drug Regimen | MICs | | |
|---|---|---|---|---|
| | | ATM | ATM/CAZ/AVI | CAZ/AVI |
| CDI694 (Post-Exposure) | **Growth Control** | >64 | ≤0.5/8/4 | 1/4 |
| | **100% CAZ/AVI** | >64 | ≤0.5/8/4 | 2/4 |
| | **10% CAZ/AVI** | >64 | ≤0.5/8/4 | 2/4 |
| CDI231 (Post-Exposure) | **Growth Control** | >64 | ≤0.5/8/4 | >64/4 |
| | **100% CAZ/AVI + ATM** | >64 | ≤0.5/8/4 | >64/4 |
| | **10% CAZ/AVI + ATM** | >64 | ≤0.5/8/4 | >64/4 |

ATM, aztreonam; CAZ/AVI, ceftazidime/avibactam.

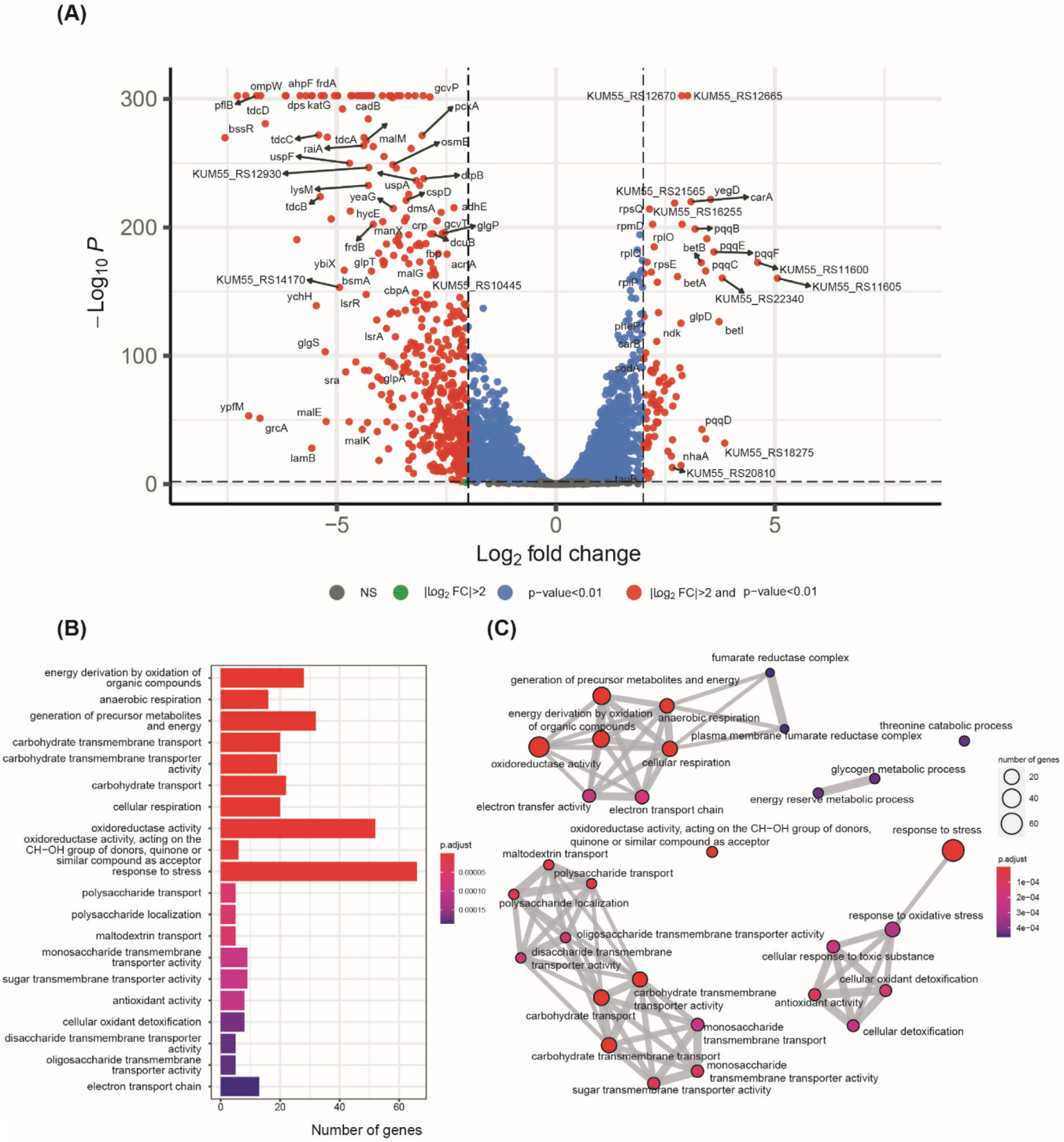


**Fig. 4.** RNAseq analysis of CDI231 following exposure to CAZ/AVI in combination with ATM for 48 h. Volcano plot of differentially expressed genes (A). Barplot of gene ontology (GO) enrichment analysis of differentially expressed genes (DEGs) (B). Interaction networks between top 30 enriched GOs (C).

CDI231, respectively. However, these regimens failed to eradicate either of the isolates. Transcriptomic analysis identified genes in multiple pathways that were perturbed following antibiotic exposure such as generation of energy/respiration, carbohydrate transport, and stress response, suggesting they may contribute to antibiotic tolerance in CR-hvKP.

Against CDI694 (harbors $bla_{KPC-2}$), CAZ/AVI was bactericidal in the time-kill assays, but no synergy was detected with other antibiotics. Using MIC testing, we previously showed that CAZ/AVI remains highly active against KPC-producing CR-hvKP isolates.[15,44] However, to our knowledge this is the first *in vitro* study to further investigate the pharmacodynamic activity of CAZ/AVI-based regimens against CR-KP isolates with clearly defined hypervirulence genes. Interestingly, we observed somewhat limited bacterial killing by CAZ/AVI in the dynamic one-compartment PK/PD model (~2 $\log_{10}$cfu/mL reduction was observed at 48 h). Some previous studies against KPC-producing *K. pneumoniae* isolates in dynamic PK/PD models showed more

**Table 3**
Differentially expressed hypervirulence or β-lactam-resistance genes in CDI231 following exposure to CAZ/AVI and ATM in the one-compartment model. A $\log_2$ fold change cutoff of < −1 or > 1 with a false discovery rate (FDR) adjusted *P* value of < 0.05 was applied.

| | Differentially Expressed Gene | Gene Product | Locus Tag | $\log_2$ Fold-Change |
|---|---|---|---|---|
| Genes Associated with Hypervirulence [1] | *galF* | cps region; UTP–glucose-1-phosphate uridylyltransferase | KUM55_RS08335 | −1.45 |
| | *rmpA* | regulator of mucoid phenotype A | KUM55_RS28055 | −1.54 |
| | *peg-589* | putative carboxymuconolactone decarboxylase family | KUM55_RS28210 | −1.32 |
| | *iucB* | N(6)-hydroxylysine O-acetyltransferase IucB | KUM55_RS28175 | 1.13 |
| | *iucD* | NADPH-dependent L-lysine N(6)-monooxygenase | KUM55_RS28185 | 1.12 |
| Genes Associated with β-lactam-Resistance [2] | $bla_{\text{SHV-110}}$ | β-lactamase SHV-110 | KUM55_RS13745 | −2.44 |
| | $bla_{\text{OXA-48}}$ | β-lactamase OXA-48 | KUM55_RS26355 | −1.05 |
| | *ompK36* | Outer membrane porin OmpK36 | KUM55_RS07720 | −1.18 |
| | *ompW* | Outer membrane protein W | KUM55_RS15220 | −6.74 |

[1] Other hypervirulence associated genes that did not display significant differences in expression include: *iucA, dltA, terB, peg-344,* and other genes in the cps coding region (KUM55_RS08335-KUM55_RS08420).
[2] Other β-lactam-resistance and permeability associated genes that did not display significant differences in expression include: $bla_{\text{NDM}}$, $bla_{\text{OXA-1}}$, *ompK26, ompK35, ompK37, lamB_2, lamB_3, ompX, oprM, tolC, phoE.*

killing than we observed in the present study (>5 $\log_{10}$cfu/mL killing by 48 h),[45,46] while our previous data suggest inter-isolate variations in the rate of killing exist (between 2.5 and 5 $\log_{10}$cfu/mL killing by 48 h).[47] However, isolates from the previous *in vitro* studies were from ST258, were not identified as hypervirulent, and they had lower MICs to CAZ/AVI ranging from 0.125/4 to 0.5/4mg/L (MICs in present study, 4/4mg/L).

Against CDI231 (harbors $bla_{\text{OXA-48}}$ and $bla_{\text{NDM-1}}$), the time-kill assays showed that no monotherapies were bactericidal and combinations with CAZ/AVI + ATM were synergistic. Previous time-kill studies also detected synergy between CAZ/AVI + ATM against non-hypervirulent *K. pneumoniae* strains that harbored NDM-1 and/or OXA.[48,49] Similar to the response of CDI694 to CAZ/AVI, CDI231 persisted despite exposure to CAZ/AVI + ATM in the one-compartment model. In contrast, a previous study by Lodise *et al* using the hollow fiber infection model showed more rapid bacterial killing for CAZ/AVI + ATM against a non-hypervirulent *K. pneumoniae* with $bla_{\text{NDM-1}}$ (ATM/CAZ/AVI MIC = 2/8/4mg/L).[50] However, like our study, Lodise *et al* also found that CAZ/AVI + ATM against an *Escherichia coli* isolate with $bla_{\text{NDM-1}}$ (ATM/CAZ/AVI MIC = 4/8/4mg/L) failed to demonstrate bactericidal activity through 168 h. Since both isolates in the study by Lodise *et al* had MICs that varied by only 1 dilution and the MIC to ATM/CAZ/AVI for CDI231 was $\leq$ 0.5/8/4mg/L, MIC differences alone are not likely to explain the variations in pharmacodynamic response to CAZ/AVI + ATM.

Interestingly, the failure of CAZ/AVI-based regimens to eradicate the CR-hvKP isolates was not caused by the development of a stable resistant population. CR-hvKP isolates did not display increased MICs following antibiotic exposure. Thus, the transcriptomic response of CDI231 was evaluated to help identify potential mechanisms the isolate used to persist during CAZ/AVI + ATM therapy. One notable outer membrane porin, *ompW*, was significantly downregulated. Although β-lactams primarily enter *K. pneumoniae* through *ompK35* and *ompK36*, altered expression of OmpW has been detected during antibiotic-exposure, including to β-lactams.[51,52] However, it is not likely that this porin directly permits passage of ceftazidime or aztreonam,[53] so its role in antibiotic tolerance may be indirect in the present study. Decreased expression of some β-lactamase genes ($bla_{\text{SHV-110}}$ and $bla_{\text{OXA-48}}$) after 48 h of antibiotic exposure were noted and may also suggest that CDI231 was able to adapt to repel antibiotic penetration. However, other β-lactamase genes ($bla_{\text{NDM}}$ and $bla_{\text{OXA-1}}$) were not differentially expressed.

Various genes that are involved in the cellular respiration and energy pathways were also downregulated in CDI231 during antibiotic exposure, suggesting a relationship between cell respiration and antibiotic tolerance. Low *et al* also found a suppression of genes involved in the tricarboxylic acid cycle in NDM-producing *K. pneumoniae* following exposure to β-lactams.[54] Decreased metabolic activity in cells has been linked to the formation of bacterial persisters, which can be antibiotic tolerant.[55] One series of genes that were perturbed in CDI231 was the *frdABCD* operon, which encodes a fumarate reductase enzyme that is part of the anaerobic respiration pathway that converts fumarate to succinate. The downregulation of fumarases encoded by *fumA* and *fumB* also suggest that fumarate is important for antibiotic tolerance in this *K. pneumoniae* isolate. The *frdABCD* operon was downregulated with antibiotic exposure in the CDI231 cells and may have led to accumulation of fumarate. Previously, Kim *et al* showed that fumarate accumulation in *E. coli* led to ampicillin and norfloxacin tolerance.[56] However, in contrast to the present study, they also showed that overexpression of *frd*, particularly in the presence of exogenous fumarate, further potentiated antibiotic tolerance in *E. coli* by using fumarate as a terminal electron acceptor in anaerobic respiration. It is possible that in *K. pneumoniae* CDI231, fumarate accumulation instead facilitated antibiotic tolerance by depleting intracellular glycerol-3-phosphate (G3P) concentrations through the activation of the anaerobic glycerol-3-phosphate dehydrogenase.[57] Decreased G3P may increase persistence and prevent bacteria from resuscitating to a metabolically active (and more sensitive) growth state.[58] Furthermore, the aerobic glycerol-3-phosphate dehydrogenase gene (*glpD*), which encodes an enzyme that metabolizes the conversion of G3P to the glycolysis metabolite dihydroxyacetone phosphate, was upregulated in CDI231 during antibiotic exposure and may also lead to decreased intracellular G3P. Upregulation of *glpD* has previously been identified in *E. coli* persisters that were tolerant to ampicillin and ofloxacin.[58,59] Taken together, antibiotic tolerance may in part be due to a decrease in the intracellular concentration of G3P that occurs through multiple pathways.

There was also a consistent pattern of decreased expression of genes encoding carbohydrate transport proteins. For example, the *lamB* gene encoding maltoporin was significantly downregulated. LamB functions to import maltose and maltodextrins. Reduced expression of this protein has been observed in tetracycline- and fluoroquinolone-resistant *E. coli*, which may be due to reduced penetration of these antibiotics directly through this porin.

[60,61] Reduced expression of LamB has also been observed following exposure to colistin.[62] However, it has been shown that LamB does not permit significant penetration of the β-lactams to the bacterial periplasm in *K. pneumoniae*.[63] Thus, LamB's decreased expression in CDI231 in the present study may be a general bacterial defense to antibiotic exposure. Similarly, the expression of other genes involved in carbohydrate transport, such as *malE, malF, malG, malK,* and *manXYZ*, were depressed following antibiotic exposure. Further studies are required to determine if these alterations directly contribute to resistance in *K. pneumoniae*.

The expression of bacterial stress response genes in CDI231 were generally downregulated in the presence of antibiotics. Indeed, it has been suggested that antibiotic exposure by bactericidal antibiotics, such as the β-lactams, can induce redox stress through reactive oxygen species (ROS) such as $H_2O_2$, though this remains controversial.[64] Interestingly, most $H_2O_2$-scavenger encoding genes were significantly downregulated (*ahpC, ahpF, katE,* and *katG*) compared to the unexposed control. Some previous studies have found that the catalase-peroxidase *katG* was upregulated with antibiotic exposure[65] while others have shown that it was downregulated or unaffected.[64,66] It remains unclear why the $H_2O_2$-scavenger encoding genes were downregulated but it is possible that bacterial cells displaying higher $H_2O_2$ levels displayed increased persistence, as has been observed in *E. coli*.[67] Additional bacterial stress and cold/heat shock responses were also downregulated following 48 h of antibiotic exposure. Many studies have found that the stress response genes are activated following antibiotic exposure,[68] although it may also depend on the duration of antibiotic exposure. For example, an NDM-producing *K. pneumoniae* isolate exposed to chloramphenicol initially upregulated some stress response genes but they were significantly downregulated by 4 h.[69] Thus, in the present study, where the transcriptomic response was evaluated after 48 h, it is possible that the need for a stress response diminishes as the cells become quiescent.

One notable limitation of this study is that the definition of hypervirulence was based on the bacterial genotype. Future animal experiments are required to validate the hypervirulence phenotype in these isolates. However, the genetic biomarkers for hypervirulence used in this study are generally effective to differentiate hvKP from cKP.[2] Another limitation was that RNA-seq was only performed on samples exposed to antibiotics for 48 h. It is likely that the transcriptomic response varies over time.

In summary, CAZ/AVI-based regimens were active against CR-KP isolates with hypervirulence genes but failed to eradicate either isolate by 48 h. Synergy was not observed for any antibiotic in combination with CAZ/AVI for CDI694, while synergy between CAZ/AVI + ATM was detected against CDI231. Transcriptomic analyses suggested that perturbations to multiple pathways, including cell respiration, carbohydrate transport, and stress response, may have enabled CDI231 to survive despite β-lactam concentrations well above the MIC. Furthermore, expression of genes associated with hypervirulence and antibiotic resistance were generally not strongly impacted by drug exposure with the exception of *ompW,* which was significantly downregulated. Elucidation of mechanisms that cause antibiotic tolerance may lead to optimized antibiotic combinations that can suppress these adaptations. Additional studies are warranted that can elucidate antibiotic regimens capable of extensive bacterial killing against CR-hvKP to combat this emerging threat.

## Declaration of Competing Interest

The authors declare that they have no known competing financial interests or personal relationships that could have appeared to influence the work reported in this paper.

## Funding

This work was in part supported by grants from the National Institutes of Health (NIH) to BK and LC (R01AI090155) and to ZB, BK, and LC (R01AI148560). The content of this manuscript is solely the responsibility of the authors and does not necessarily represent the official views of the NIH.

## Appendix A. Supplementary data

Supplementary data to this article can be found online at https://doi.org/10.1016/j.ijtst.2018.11.001.

## References

[1] Podschun R, Ullmann U. Klebsiella spp. as nosocomial pathogens: epidemiology, taxonomy, typing methods, and pathogenicity factors. Clin Microbiol Rev 1998;11:589–603.
[2] Russo TA et al. Identification of Biomarkers for Differentiation of Hypervirulent Klebsiella pneumoniae from Classical K. pneumoniae. *J Clin Microbiol* **56** 2018. https://doi.org/10.1128/JCM.00776-18.
[3] Boucher HW et al. Bad bugs, no drugs: no ESKAPE! An update from the Infectious Diseases Society of America. Clin Infect Dis 2009;48:1–12. https://doi.org/10.1086/595011.
[4] Sui W et al. Whole genome sequence revealed the fine transmission map of carbapenem-resistant Klebsiella pneumonia isolates within a nosocomial outbreak. Antimicrob Resist Infect Control 2018;7:70. https://doi.org/10.1186/s13756-018-0363-8.
[5] Decre D et al. Emerging severe and fatal infections due to Klebsiella pneumoniae in two university hospitals in France. J Clin Microbiol 2011;49:3012–4. https://doi.org/10.1128/JCM.00676-11.
[6] Li J et al. Risk factors and clinical outcomes of hypervirulent Klebsiella pneumoniae induced bloodstream infections. Eur J Clin Microbiol Infect Dis 2018;37:679–89. https://doi.org/10.1007/s10096-017-3160-z.
[7] Fang CT et al. Klebsiella pneumoniae genotype K1: an emerging pathogen that causes septic ocular or central nervous system complications from pyogenic liver abscess. Clin Infect Dis 2007;45:284–93. https://doi.org/10.1086/519262.
[8] Paczosa MK, Mecsas J. Klebsiella pneumoniae: Going on the Offense with a Strong Defense. Microbiol Mol Biol Rev 2016;80:629–61. https://doi.org/10.1128/MMBR.00078-15.
[9] Russo TA, Marr CM. Hypervirulent Klebsiella pneumoniae. Clin Microbiol Rev 2019;32. https://doi.org/10.1128/cmr.00001-19.
[10] Siu LK, Yeh KM, Lin JC, Fung CP, Chang FY. Klebsiella pneumoniae liver abscess: a new invasive syndrome. Lancet Infect Dis 2012;12:881–7. https://doi.org/10.1016/S1473-3099(12)70205-0.
[11] Zhang Y et al. Evolution of hypervirulence in carbapenem-resistant Klebsiella pneumoniae in China: a multicentre, molecular epidemiological analysis. J Antimicrob Chemother 2020;75:327–36. https://doi.org/10.1093/jac/dkz446.
[12] Cejas D et al. First isolate of KPC-2-producing Klebsiella pneumonaie sequence type 23 from the Americas. J Clin Microbiol 2014;52:3483–5. https://doi.org/10.1128/JCM.00726-14.
[13] Karlsson M et al. Identification of a Carbapenemase-Producing Hypervirulent Klebsiella pneumoniae Isolate in the United States. Antimicrob Agents Chemother 2019;63. https://doi.org/10.1128/AAC.00519-19.
[14] Gu D et al. A fatal outbreak of ST11 carbapenem-resistant hypervirulent Klebsiella pneumoniae in a Chinese hospital: a molecular epidemiological study. Lancet Infect Dis 2018;18:37–46. https://doi.org/10.1016/S1473-3099(17)30489-9.
[15] Yu F et al. In Vitro Activity of Ceftazidime-Avibactam against Carbapenem-Resistant and Hypervirulent Klebsiella pneumoniae Isolates. Antimicrob Agents Chemother 2018;62. https://doi.org/10.1128/AAC.01031-18.
[16] van Duin D et al. Colistin Versus Ceftazidime-Avibactam in the Treatment of Infections Due to Carbapenem-Resistant Enterobacteriaceae. Clin Infect Dis 2018;66:163–71. https://doi.org/10.1093/cid/cix783.
[17] Falcone M et al. Efficacy of ceftazidime-avibactam plus aztreonam in patients with bloodstream infections caused by MBL- producing Enterobacterales. Clin Infect Dis 2020. https://doi.org/10.1093/cid/ciaa586.
[18] Campos MA et al. Capsule polysaccharide mediates bacterial resistance to antimicrobial peptides. Infect Immun 2004;72:7107–14. https://doi.org/10.1128/iai.72.12.7107-7114.2004.
[19] Liu H, Zhu M, Zhu S. Persistence of Antibiotic Resistance and Capsule in E. coli B23 after Removal from Sublethal Kanamycin Treatment. *Journal of Experimental.* Microbiol Immunol 2011;15:43–6.
[20] Ganal S, Gaudin C, Roensch K, Tran M. Effects of streptomycin and kanamycin on the production of capsular polysaccharides in Escherichia coli B23 cells. Journal of Experimental Microbiology and Immunology 2007;11:54–9.
[21] Geisinger E, Isberg RR. Antibiotic modulation of capsular exopolysaccharide and virulence in Acinetobacter baumannii. PLoS Pathog 2015;11:e1004691.
[22] Chen L, Kreiswirth BN. Convergence of carbapenem-resistance and hypervirulence in *Klebsiella pneumoniae*. Lancet Infect Dis 2018;18:2–3. https://doi.org/10.1016/s1473-3099(17)30517-0.

[23] Wick RR, Judd LM, Gorrie CL, Holt KE. Unicycler: Resolving bacterial genome assemblies from short and long sequencing reads. PLoS Comput Biol 2017;13:e1005595.
[24] CLSI. Performance standards for antimicrobial susceptibility testing. CLSI supplement M100–29. 29th edn,, 2019.
[25] Huang Y et al. *In vitro* Optimization of Ceftazidime/Avibactam for KPC-Producing *Klebsiella pneumoniae*. Front Microbiol 2021;12:. https://doi.org/10.3389/fmicb.2021.618087618087.
[26] Butler DA et al. Optimizing aminoglycoside selection for KPC-producing *Klebsiella pneumoniae* with the aminoglycoside-modifying enzyme (AME) gene *aac(6')-Ib*. J Antimicrob Chemother 2021;76:671–9. https://doi.org/10.1093/jac/dkaa480.
[27] Ramirez MS, Nikolaidis N, Tolmasky ME. Rise and dissemination of aminoglycoside resistance: the *aac(6')-Ib* paradigm. Front Microbiol 2013;4:121. https://doi.org/10.3389/fmicb.2013.00121.
[28] Casin I et al. Aminoglycoside 6'-N-acetyltransferase variants of the Ib type with altered substrate profile in clinical isolates of Enterobacter cloacae and Citrobacter freundii. Antimicrob Agents Chemother 1998;42:209–15.
[29] Jousset AB et al. A 4.5-Year Within-Patient Evolution of a Colistin-Resistant Klebsiella pneumoniae Carbapenemase-Producing K. pneumoniae Sequence Type 258. Clin Infect Dis 2018;67:1388–94. https://doi.org/10.1093/cid/ciy293.
[30] Guillard T et al. Ciprofloxacin treatment failure in a murine model of pyelonephritis due to an AAC(6')-Ib-cr-producing Escherichia coli strain susceptible to ciprofloxacin in vitro. Antimicrob Agents Chemother 2013;57:5830–5. https://doi.org/10.1128/aac.01489-13.
[31] Tsuji BT et al. International Consensus Guidelines for the Optimal Use of the Polymyxins: Endorsed by the American College of Clinical Pharmacy (ACCP), European Society of Clinical Microbiology and Infectious Diseases (ESCMID), Infectious Diseases Society of America (IDSA), International Society for Anti-infective Pharmacology (ISAP), Society of Critical Care Medicine (SCCM), and Society of Infectious Diseases Pharmacists (SIDP). Pharmacotherapy 2019;39:10–39. https://doi.org/10.1002/phar.2209.
[32] Bolger AM, Lohse M, Usadel B. Trimmomatic: a flexible trimmer for Illumina sequence data. Bioinformatics 2014;30:2114–20. https://doi.org/10.1093/bioinformatics/btu170.
[33] Langmead B, Salzberg SL. Fast gapped-read alignment with Bowtie 2. Nat Methods 2012;9:357–9. https://doi.org/10.1038/nmeth.1923.
[34] Anders S, Pyl PT, Huber W. HTSeq–a Python framework to work with high-throughput sequencing data. Bioinformatics 2015;31:166–9. https://doi.org/10.1093/bioinformatics/btu638.
[35] Love MI, Huber W, Anders S. Moderated estimation of fold change and dispersion for RNA-seq data with DESeq2. Genome Biol 2014;15:550. https://doi.org/10.1186/s13059-014-0550-8.
[36] Huerta-Cepas J et al. eggNOG 5.0: a hierarchical, functionally and phylogenetically annotated orthology resource based on 5090 organisms and 2502 viruses D314. Nucleic Acids Res 2019;47:D309. https://doi.org/10.1093/nar/gky1085.
[37] Kanehisa M, Sato Y, Morishima K. BlastKOALA and GhostKOALA: KEGG Tools for Functional Characterization of Genome and Metagenome Sequences. J Mol Biol 2016;428:726–31. https://doi.org/10.1016/j.jmb.2015.11.006.
[38] Yu G, Wang LG, Han Y, He QY. clusterProfiler: an R package for comparing biological themes among gene clusters. OMICS 2012;16:284–7. https://doi.org/10.1089/omi.2011.0118.
[39] Wang Q et al. Phenotypic and Genotypic Characterization of Carbapenem-resistant Enterobacteriaceae: Data From a Longitudinal Large-scale CRE Study in China (2012–2016). Clin Infect Dis 2018;67:S196–205. https://doi.org/10.1093/cid/ciy660.
[40] Mukherjee S et al. Emergence of OXA-232-producing hypervirulent Klebsiella pneumoniae ST23 causing neonatal sepsis. J Antimicrob Chemother 2020. https://doi.org/10.1093/jac/dkaa080.
[41] Pajand O et al. The emergence of the hypervirulent Klebsiella pneumoniae (hvKp) strains among circulating clonal complex 147 (CC147) harbouring blaNDM/OXA-48 carbapenemases in a tertiary care center of Iran. Ann Clin Microbiol Antimicrob 2020;19:12. https://doi.org/10.1186/s12941-020-00349-z.
[42] Roulston KJ, Bharucha T, Turton JF, Hopkins KL, Mack DJF. A case of NDM-carbapenemase-producing hypervirulent Klebsiella pneumoniae sequence type 23 from the UK. JMM Case Rep 2018;5:e005130.
[43] Compain F et al. Primary osteomyelitis caused by an NDM-1-producing K. pneumoniae strain of the highly virulent sequence type 23. *Emerg*. Microbes Infect 2017;6:e57.
[44] Hao M et al. In vitro Activity of Apramycin Against Carbapenem-Resistant and Hypervirulent *Klebsiella pneumoniae* Isolates. Front Microbiol 2020;11:425. https://doi.org/10.3389/fmicb.2020.00425.
[45] Barber KE, Pogue JM, Warnock HD, Bonomo RA, Kaye KS. Ceftazidime/avibactam versus standard-of-care agents against carbapenem-resistant Enterobacteriaceae harbouring blaKPC in a one-compartment pharmacokinetic/pharmacodynamic model. J Antimicrob Chemother 2018;73:2405–10. https://doi.org/10.1093/jac/dky213.
[46] Drusano GL et al. Pharmacodynamics of Ceftazidime plus Avibactam against KPC-2-Bearing Isolates of Klebsiella pneumoniae in a Hollow Fiber Infection Model. Antimicrob Agents Chemother 2019;63. https://doi.org/10.1128/AAC.00462-19.
[47] Huang Y et al. Generating Genotype-Specific Aminoglycoside Combinations with Ceftazidime/Avibactam for KPC-Producing *Klebsiella pneumoniae*. Antimicrob Agents Chemother 2021;65:e0069221.
[48] Biagi M et al. Searching for the Optimal Treatment for Metallo- and Serine-beta-Lactamase Producing Enterobacteriaceae: Aztreonam in Combination with Ceftazidime-avibactam or Meropenem-vaborbactam. Antimicrob Agents Chemother 2019. https://doi.org/10.1128/AAC.01426-19.
[49] Marshall S et al. Can Ceftazidime-Avibactam and Aztreonam Overcome beta-Lactam Resistance Conferred by Metallo-beta-Lactamases in Enterobacteriaceae? Antimicrob Agents Chemother 2017;61. https://doi.org/10.1128/AAC.02243-16.
[50] Lodise TP et al. Determining the optimal dosing of a novel combination regimen of ceftazidime/avibactam with aztreonam against NDM-1-producing Enterobacteriaceae using a hollow-fibre infection model. J Antimicrob Chemother 2020. https://doi.org/10.1093/jac/dkaa197.
[51] Tiwari V, Vashistt J, Kapil A, Moganty RR. Comparative proteomics of inner membrane fraction from carbapenem-resistant Acinetobacter baumannii with a reference strain. PLoS ONE 2012;7:e39451.
[52] Lin XM, Yang JN, Peng XX, Li H. A novel negative regulation mechanism of bacterial outer membrane proteins in response to antibiotic resistance. J Proteome Res 2010;9:5952–9. https://doi.org/10.1021/pr100740w.
[53] Hong H, Patel DR, Tamm LK, van den Berg B. The outer membrane protein OmpW forms an eight-stranded beta-barrel with a hydrophobic channel. J Biol Chem 2006;281:7568–77. https://doi.org/10.1074/jbc.M512365200.
[54] Low YM et al. Elucidating the survival and response of carbapenem resistant Klebsiella pneumoniae after exposure to imipenem at sub-lethal concentrations. Pathog Glob Health 2018;112:378–86. https://doi.org/10.1080/20477724.2018.1538281.
[55] Amato SM et al. The role of metabolism in bacterial persistence. Front Microbiol 2014;5:70. https://doi.org/10.3389/fmicb.2014.00070.
[56] Kim JS et al. Fumarate-Mediated Persistence of Escherichia coli against Antibiotics. Antimicrob Agents Chemother 2016;60:2232–40. https://doi.org/10.1128/aac.01794-15.
[57] Zhu MM, Lawman PD, Cameron DC. Improving 1,3-propanediol production from glycerol in a metabolically engineered Escherichia coli by reducing accumulation of sn-glycerol-3-phosphate. Biotechnol Prog 2002;18:694–9. https://doi.org/10.1021/bp020281+.
[58] Spoering AL, Vulic M, Lewis K. GlpD and PlsB participate in persister cell formation in Escherichia coli. J Bacteriol 2006;188:5136–44. https://doi.org/10.1128/jb.00369-06.
[59] Shah D et al. Persisters: a distinct physiological state of *E. coli*. BMC Microbiol 2006;6:53. https://doi.org/10.1186/1471-2180-6-53.
[60] Lin XM, Yang MJ, Li H, Wang C, Peng XX. Decreased expression of LamB and Odp1 complex is crucial for antibiotic resistance in Escherichia coli. J Proteomics 2014;98:244–53. https://doi.org/10.1016/j.jprot.2013.12.024.
[61] Xu C et al. Analysis of outer membrane proteome of Escherichia coli related to resistance to ampicillin and tetracycline. Proteomics 2006;6:462–73. https://doi.org/10.1002/pmic.200500219.
[62] Sun L et al. Proteomic Changes of Klebsiella pneumoniae in Response to Colistin Treatment and crrB Mutation-Mediated Colistin Resistance. Antimicrob Agents Chemother 2020;64. https://doi.org/10.1128/aac.02200-19.
[63] Rocker, A. *et al.* Global Trends in Proteome Remodeling of the Outer Membrane Modulate Antimicrobial Permeability in Klebsiella pneumoniae. *mBio* **11**, 10.1128/mBio.00603-20 (2020).
[64] Dwyer DJ et al. Antibiotics induce redox-related physiological alterations as part of their lethality E2109. Proc Natl Acad Sci U S A 2014;111:E2100. https://doi.org/10.1073/pnas.1401876111.
[65] Liu Y, Imlay JA. Cell death from antibiotics without the involvement of reactive oxygen species. Science 2013;339:1210–3. https://doi.org/10.1126/science.1232751.
[66] Jousset AB et al. Transcriptional Landscape of a bla (KPC-2) Plasmid and Response to Imipenem Exposure in Escherichia coli TOP10. Front Microbiol 2018;9:2929. https://doi.org/10.3389/fmicb.2018.02929.
[67] Wang T, El Meouche I, Dunlop MJ. Bacterial persistence induced by salicylate via reactive oxygen species. Sci Rep 2017;7:43839. https://doi.org/10.1038/srep43839.
[68] Harms A, Maisonneuve E, Gerdes K. Mechanisms of bacterial persistence during stress and antibiotic exposure. Science 2016;354. https://doi.org/10.1126/science.aaf4268.
[69] Abdul Rahim N et al. Transcriptomic responses of a New Delhi metallo-β-lactamase-producing Klebsiella pneumoniae isolate to the combination of polymyxin B and chloramphenicol. Int J Antimicrob Agents 2020;56:. https://doi.org/10.1016/j.ijantimicag.2020.106061106061.